

Excited states in ^{31}S studied via beta decay of ^{31}Cl

A. Kankainen^{1,a}, T. Eronen¹, S.P. Fox², H.O.U. Fynbo³, U. Hager¹, J. Hakala¹, J. Huikari¹, D.G. Jenkins², A. Jokinen¹, S. Kopecky¹, I. Moore¹, A. Nieminen¹, H. Penttilä¹, S. Rinta-Antila¹, O. Tengblad⁴, Y. Wang¹, and J. Äystö¹

¹ Department of Physics, P.O. Box 35, FI-40014 University of Jyväskylä, Finland

² Department of Physics, University of York, Heslington, York YO105DD, UK

³ Department of Physics and Astronomy, University of Aarhus, DK-8000 Aarhus C, Denmark

⁴ Instituto de Estructura de la Materia, CSIC, Serrano 113 bis, E-28006, Madrid, Spain

Received: 17 October 2005 / Revised version: 3 February 2006 /

Published online: 17 February 2006 – © Società Italiana di Fisica / Springer-Verlag 2006

Communicated by C. Signorini

Abstract. The beta decay of ^{31}Cl has been studied with a silicon detector array and a HPGe detector at the IGISOL facility. Previously controversial proton peaks have been confirmed to belong to ^{31}Cl and a new proton group with an energy of 762(14) keV has been found. Proton captures to this state at 6921(15) keV in ^{31}S can have an effect on the reaction rate of $^{30}\text{P}(p,\gamma)$ in ONe novae. Gamma rays of 1249.1(14) keV and 2234.5(8) keV corresponding to the de-excitations of the first two excited states in ^{31}S have been measured. No beta-delayed protons from the IAS have been observed.

PACS. 23.20.Lv γ transitions and level energies – 23.50.+z Decay by proton emission – 27.30.+t $20 \leq A \leq 38$ – 29.30.Ep Charged-particle spectroscopy

1 Introduction

Beta decays of odd- Z , $T_Z = -3/2$ nuclei, such as ^{31}Cl , are characterised by a strong superallowed beta decay to the isobaric analogue state (IAS) in the daughter nucleus and Gamow-Teller (GT) transitions to states both below and above the IAS. A set of strong GT transitions above the IAS, the so-called giant GT resonance, is also typical for nuclei of this kind. A relatively large Q_{EC} -value of 11980(50) keV [1], measured in $^{36}\text{Ar}(^3\text{He},^8\text{Li})^{31}\text{Cl}$ reactions [2], provides an opportunity to study beta decay strength of ^{31}Cl over a broad energy range. A comparison of the experimental strength to the strength obtained via sd -shell model calculations can be used to test the shell model. Nevertheless, beta decays of $T_Z = -3/2$ nuclei are not known very well due to weak proton decay branches resulting from high binding energies for protons in daughter nuclei. Sometimes it can even be challenging to observe a strong beta decay to the IAS. For instance, the IAS at 6268(10) keV [3] lies just above the proton separation energy in ^{31}S , $S_p = 6133.0(15)$ keV [1], and decays most likely by emitting low-energy protons or high-energy gamma rays which are hard to detect.

The beta decay of ^{31}Cl has been studied previously by He-jet method (see refs. [4–7]). A half-life of 150 ± 25 ms

has been determined from the most intense proton peak at 989 keV in [4]. Proton groups at 989(15) keV and 1528(20) keV have been reported in [5] and six additional proton peaks have been observed in the energy range of 845 keV–2204 keV in [6]. The beta branching of the 986 keV protons has been estimated to be 0.44% and the total branching of proton-emitting states to be 0.7% in [6]. Although several proton peaks have been carefully measured, the experiments have suffered from the lack of mass separation. For example, all peaks except those of 986 keV and 1520 keV observed in [6] have later been claimed to arise from the beta decay of ^{29}Si [7]. In addition, beta-delayed protons from ^{32}Cl have dominated the spectra which has made it difficult to distinguish possible weak proton peaks of ^{31}Cl . No beta-delayed γ -rays have been observed in these experiments. Nevertheless, one γ -ray has been associated with the beta decay of ^{31}Cl in an experiment on the beta decay of ^{31}Ar [8]. This 2235.5(5) keV gamma ray corresponds to the decay of the second excited state ($5/2^+$) to the ground state of ^{31}S ($1/2^+$).

The beta decay of ^{31}Cl leads to states in ^{31}S whose energies and decay properties are intrinsically interesting in respect of the opportunity to study the mirror energy differences between these states and those in the mirror nucleus, ^{31}P . A recent experiment studied the excited states of ^{31}S and ^{31}P populated via $^{12}\text{C}(^{20}\text{Ne},n)$ and $^{12}\text{C}(^{20}\text{Ne},p)$ reactions with the Gammasphere detec-

^a e-mail: anu.kankainen@phys.jyu.fi

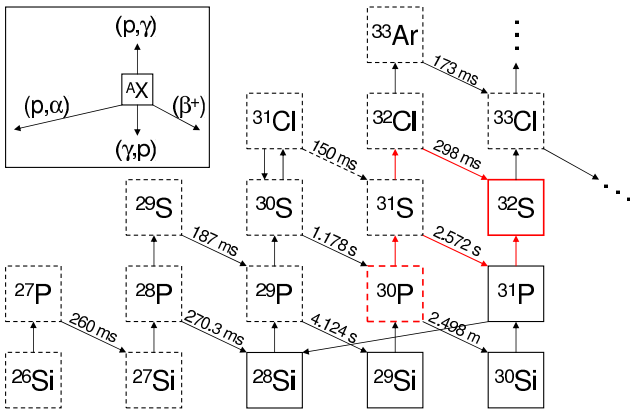


Fig. 1. Main nuclear paths in the Si-Ca mass region in ONe novae according to ref. [13]. ^{30}P is a mandatory passing point on the way to ^{32}S and heavier elements.

tor set-up at the ATLAS accelerator at Argonne National Laboratory [9]. The mirror energy differences have also been studied via one-neutron pickup reactions on ^{32}S [10] and via one- or two-nucleon transfer reactions, such as $^{29}\text{Si}(^3\text{He}, n(\gamma\gamma))^{31}\text{Si}$ [11].

Decay properties of the excited states in ^{31}S are also important for the studies of the nucleosynthesis in oxygen-neon (ONe) novae. Novae of this kind are produced by thermonuclear runaways in a binary system consisting of a white dwarf and a main-sequence companion (see refs. [12] and [13]). ONe novae contain not only CNO-group nuclei but also Ne, Na, Al and other intermediate-mass nuclei. Proton captures on these seed nuclei in the NeNa-MgAl region drive the nuclear activity up to the Si-Ca mass region [13]. Species beyond sulphur are produced via two paths, either $^{30}\text{P}(p, \gamma)^{31}\text{S}(p, \gamma)^{32}\text{Cl}(\beta^+)^{32}\text{S}$ or $^{30}\text{P}(p, \gamma)^{31}\text{S}(\beta^+)^{31}\text{P}(p, \gamma)^{32}\text{S}$ (see fig. 1). Thus, ^{30}P is a mandatory passing point and it stops further nucleosynthesis unless proton captures to the states of ^{31}S are fast enough.

Although several excited states above the proton separation energy in ^{31}S have been measured quite accurately, the spins are not known so well. Thus, more spectroscopic information is needed to estimate the $^{30}\text{P}(p, \gamma)$ rate which is presumably governed by the properties of a few individual levels in ^{31}S . José *et al.* have emphasised the importance of this reaction rate and the effects of its uncertainty in ONe novae [13]. If the rate is much higher than estimated, much less ^{30}Si is left in the envelope of a nova. On the other hand, if the rate is much lower than estimated, it will lead to an enhancement of ^{30}Si as the slow beta decay of ^{30}P can compete favourably against proton captures. This will reduce the yields of nuclei above ^{32}S significantly. The abundance pattern is important as it gives information on the underlying white dwarf. It can also explain nova origin of presolar grains and γ -rays observed from nova outbursts [13]. These outbursts spread nuclear-processed material into the interstellar medium and can therefore contribute to the Galactic nucleosynthesis.

2 Experimental method

The beta decay of ^{31}Cl was studied using the IGISOL (Ion Guide Isotope Separator On-Line) facility [14]. ^{31}Cl nuclei were produced via $^{32}\text{S}(p, 2n)$ fusion-evaporation reactions induced by a 40 MeV or 45 MeV proton beam on a ZnS target. The proton beam intensity was 10–20 μA during the experiment. For calibration purposes, ^{24}Al was produced with a 30 MeV proton beam and ^{20}Na with a 45 MeV proton beam on a Mg target. The yield of ^{31}Cl as a number of ions at the measurement set-up was about 14 s^{-1} with a 40 MeV proton beam and 12 s^{-1} with a 45 MeV proton beam. The corresponding yields of ^{31}S were $2 \times 10^4\text{ s}^{-1}$ and $1.5 \times 10^4\text{ s}^{-1}$.

The produced nuclei were accelerated to 25 keV, mass-separated and implanted into a $30\text{ }\mu\text{g}/\text{cm}^2$ thick carbon foil placed at 45° angle to the beam (see fig. 2). The beam entered the detector chamber through an aperture of the ISOLDE Silicon Ball detector array [15], which is a hemisphere consisting of 36 silicon detectors segmented in four quadrants yielding a total of 144 detectors with a size of $25.5 \times 25.5\text{ mm}^2$. In order to avoid beam hitting to the back side of the Silicon Ball detector, a collimator plate ($d = 8\text{ mm}$) was put in front of the aperture.

A 70% HPGe detector measured gamma rays. Its end cap was put into a tube going inside the detector chamber about 6.5 cm away from the implantation point. It was

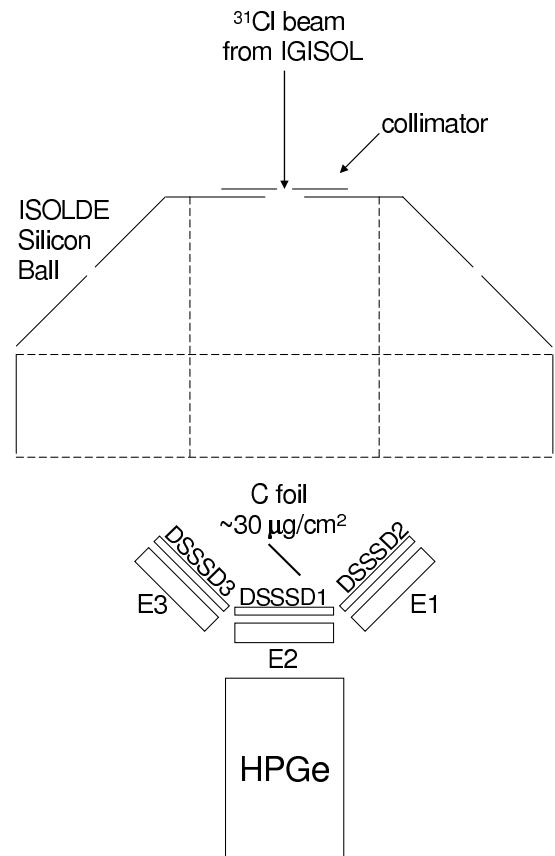


Fig. 2. The experimental set-up.

calibrated with ^{60}Co , ^{134}Cs and ^{228}Th sources and on-line with high-energy γ -rays from ^{24}Al β -decay.

The carbon foil was also surrounded by three double-sided silicon strip detectors (DSSSDs) which were backed with three thick silicon detectors. Two DSSSDs were at 45° angle with respect to the third one in order to maximise the solid angle covered by the detectors. The front side of a DSSSD consists of 16 strips (*front strips*) which are 50 mm long and 3 mm wide and separated by 0.1 mm and the back face has 16 similar but orthogonal strips (*back strips*), see refs. [16] and [17]. One of the DSSSDs was a MICRON design W detector with a dead layer of 600 nm [16]. The rest were MICRON's new thin-window designed detectors with ultra-thin dead layers of 100 nm [17]. As the DSSSDs were only about $60\ \mu\text{m}$ thick, beta particles left very little energy in them. Therefore, the DSSSDs were ideal for detecting protons and alpha particles.

The data acquisition was triggered by beta particles which meant a hit in any of the three thick silicon detectors behind the DSSSDs or a hit in any of the detectors in the Silicon Ball. The total beta efficiency was measured as 24.9(19)% based on the intensity ratio of the 1266 keV γ -peak following the beta decay of ^{31}S in a beta-triggered spectrum and in a singles spectrum. The geometrical beta efficiency was little higher, about 37.5(10)%. The data acquisition suffered from noise, which was one reason for the rejection of the silicon detectors in the outer ring of the Silicon Ball frame. As a result, only 80 Silicon Ball detectors used in the experiment were appropriate for detecting beta particles, whereas the DSSSDs served as proton detectors. Unwanted events in the DSSSDs could be rejected in the data analysis by requiring that for each event in a front strip there must be an event with a corresponding energy in one of the back strips. However, protons below 700 keV could not be observed with the DSSSDs due to noise.

The DSSSDs were calibrated in a similar manner as explained in ref. [16]. At first, the position of the source with respect to the detectors was determined and the strips were calibrated with ^{20}Na and ^{148}Gd . In order to observe low-energy protons ($E_p \approx 130\ \text{keV}$) from the IAS of ^{31}S with a good energy resolution, the amplification was set to about 1 keV/channel. Unfortunately, with this amplification we could only use 2148 keV alphas from ^{20}Na and 3183 keV alphas from the ^{148}Gd source for the calibration. Beta-delayed alphas from ^{24}Al were not intense enough to calibrate each strip individually. The energy left to the dead layer and that deposited into the detector were calculated using the stopping power and range tables from SRIM2003 [18]. For each front (back) strip a coincidence with one central back (front) strip 8 or 9 was required. There were not enough data in one pixel for energy calibration with ^{20}Na and therefore, the foil and dead energy effect were calculated as a solid-angle-weighted average for each strip.

The original energy calibration gave too low energies for protons. This was expected from the lack of low-energy calibration points, which made the errors in the peak fits and deposited energies (caused by the uncertainties in dead layers, foil thicknesses and positions of the de-

tectors) essential. The calibration was corrected with the most intense proton peak of ^{31}Cl ($E_p = 986(10)\ \text{keV}$ [6]). As this peak was not intense enough in individual strips, this was done by adding together all front strips for each DSSSD and all back strips for each DSSSD. The solid-angle-weighted average energies deposited into the detectors from the 986 keV peak were calculated and the energy calibration was corrected by adding the difference between the calculated values and the energies from the first calibration. The new calibration agreed with the earlier results for the known peaks.

3 Beta-delayed γ -rays

The isolation of beta-delayed γ -rays with the HPGe detector was experimentally challenging. Firstly, gamma spectra were dominated by the beta decay of ^{31}S which is much longer-lived ($T_{1/2} = 2.572\ \text{s}$) and produced more abundantly (see sect. 2) than ^{31}Cl . Secondly, the activity could not be removed from the set-up as the beam was continuously implanted into the carbon foil. To get an idea of ^{31}S contribution, the beam was pulsed at the switchyard of the IGISOL facility for one day. The beam was on for the first 5 s and off for the last 5 s in the total cycle of 10 seconds. The data acquisition was on from 5.5 s to 10 s which guaranteed that there was no short-lived ^{31}Cl left. The pulsed ^{31}S spectrum was scaled based on the intensities of the 511 keV annihilation peaks in the ^{31}S (pulsed) and ^{31}Cl (not pulsed) spectra and subtracted from the ^{31}Cl spectrum in order to check the peaks belonging to the beta decay of ^{31}Cl . Thirdly, beta particles detected in the silicon detector (called as E2 in fig. 2) in front of the HPGe detector triggered the data acquisition and a contribution of these beta particles is seen in the γ -spectrum (see fig. 3). This could be overcome by requiring that every time a γ -ray is detected, there is no event in the E2 silicon detector. The veto requirement revealed most of the interesting gamma peaks.

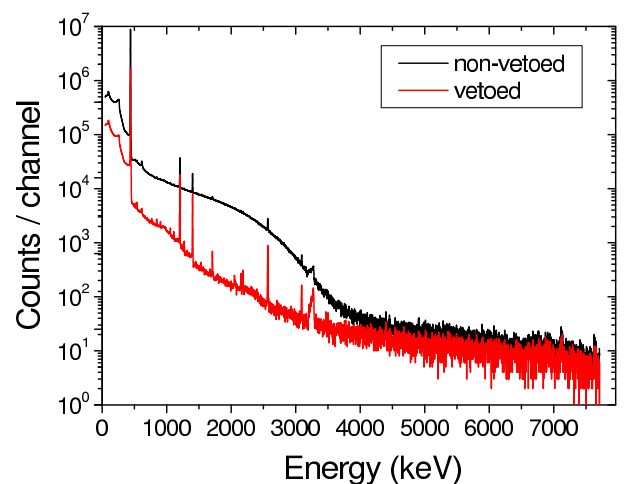


Fig. 3. A beta-triggered gamma spectrum together with a spectrum vetoed by the E2 silicon detector in front of the HPGe detector.

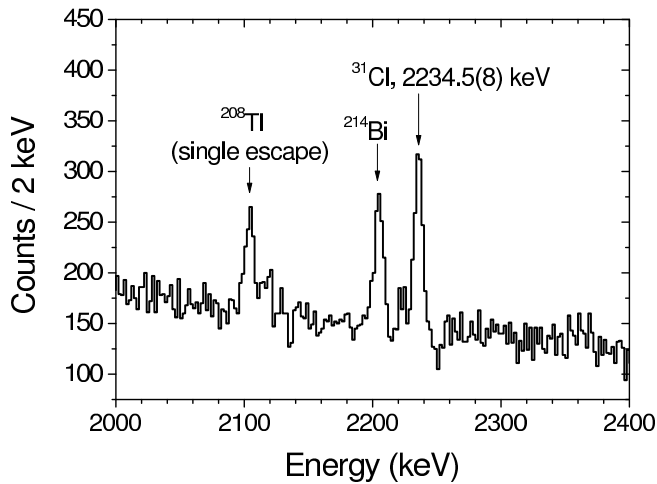


Fig. 4. The 2234.5(8) keV γ -peak in the spectrum of ^{31}Cl vetoed by the E2 silicon detector.

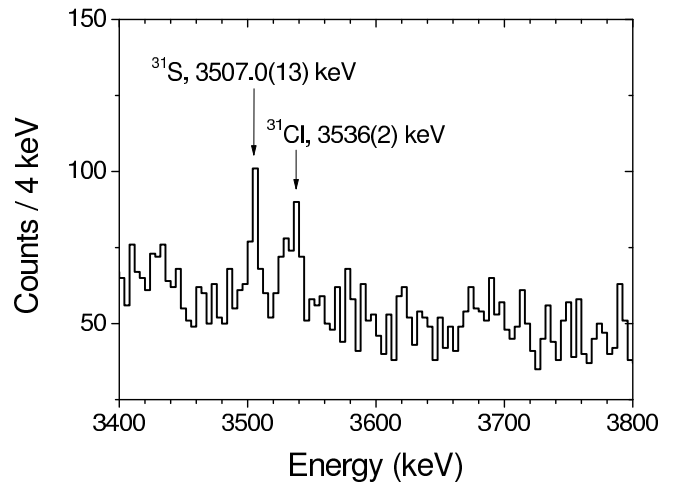


Fig. 6. The 3536(2) keV γ -peak in the spectrum of ^{31}Cl vetoed by the E2 silicon detector.

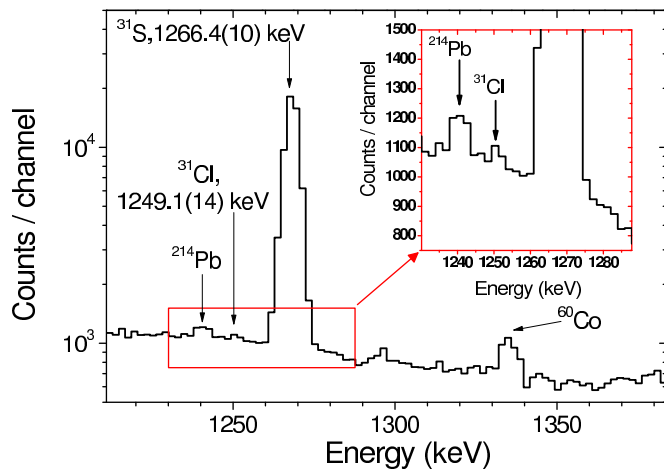


Fig. 5. The 1249.1(14) keV γ -peak in the spectrum of ^{31}Cl vetoed by the E2 silicon detector.

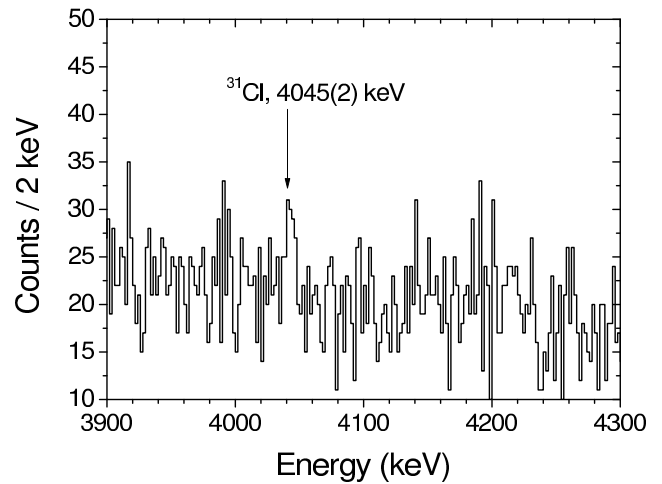


Fig. 7. The 4045(2) keV γ -peak in the spectrum of ^{31}Cl vetoed by the E2 silicon detector.

A γ -peak at an energy of 2234.5(8) keV (see fig. 4) was observed both in the spectrum where the ^{31}S contribution had been subtracted and in the spectrum vetoed by the E2 silicon detector. This peak at 2235.5(5) keV is the only γ -peak previously observed in the beta decay of ^{31}Cl [8]. As the energy gain was about 1.9 keV/channel, we could not distinguish between the 2235.5(5) keV peak of ^{31}Cl and 2239.5(6) keV peak of ^{31}S . Thus, the area of the 2239.5 keV peak was estimated based on the known γ -ray intensities and the area of the 1266.12 keV γ -peak from the beta decay of ^{31}S . Other candidates for γ -rays from the beta decay of ^{31}Cl were detected at energies of 1249.1(14) keV, 3536(2) keV and 4045(2) keV (see figs. 5, 6 and 7). These weak peaks could not be observed in the spectrum where the ^{31}S contribution had been subtracted mainly due to too low statistics in the pulsed ^{31}S spectrum.

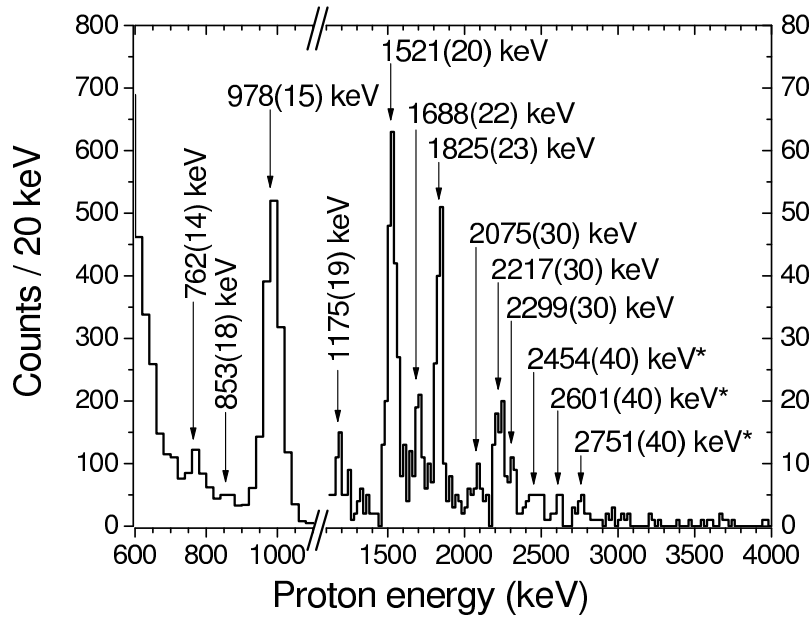
The observed gamma rays can be expected from the known levels of ^{31}S (see ref. [3] and table 1). Assuming that the γ -transition with an energy of 3536(2) keV goes to the

state at 2235.6 keV, an excitation energy of 5772(2) keV is obtained for the initial state. It agrees well with a $5/2^+$ state at 5777(5) keV in ref. [10]. If the 4045(2) keV γ -transition feeds the state at 2235.6 keV, it suggests an energy of 6280(2) keV for the IAS in ^{31}S .

Although the energy difference between the 3536(2) keV and 4045(2) keV peaks is close to 511 keV, they should not be escape peaks or sum peaks. The relative intensity of the 4045 keV transition is about 50% of the intensity of the 3536 keV transition (see table 2). Thus, the 3536 keV peak cannot be an escape peak from the 4045 keV peak. If the 4045 keV peak is due to random summing of the 511 keV γ -rays and the 3536 keV γ -rays, it would mean that about 40% of the 3536 keV γ -rays are summed with the 511 keV γ -rays. That intensive summing has not been observed with other known peaks in the spectrum, such as with the 1266 keV peak of ^{31}S .

Table 1. Observed gamma rays and corresponding literature values (from [10] for the 5777 keV state, other values from [21]).

E_γ (keV) This work	E_γ (keV) Literature	Transition
1249.1(14)	1248.8(3)	1248.9(2) keV ($3/2^+$) \rightarrow 0 keV ($1/2^+$)
2234.5(8)	2235.5(5)	2235.6(4) keV ($5/2^+$) \rightarrow 0 keV ($1/2^+$)
3536(2)	3541(5)	5777(5) keV ($5/2^+$) \rightarrow 2235.6(4) keV ($5/2^+$)
4045(2)	4032(10)	6268(10) keV ($3/2^+$, IAS) \rightarrow 2235.6(4) keV ($5/2^+$)

**Fig. 8.** Beta-delayed protons from mass-separated ^{31}Cl . The peaks marked with an asterisk are smaller than 3σ peaks.**Table 2.** The relative peak intensities from the beta decay of ^{31}Cl . The γ -peak at 2235 keV and the proton peak at 978 keV have been used for normalisation. Corresponding values from refs. [6] and [7] have been included for the known peaks. Peaks smaller than 3σ have been marked with an asterisk.

E (keV)	$I_{\gamma+p}$ (%)	I_p (%)	I_p (%) [6]	I_p (%) [7]
γ 1249.1(14)	32(7)			
γ 2234.5(8)	100(12)			
γ 3536(2)	26(8)			
γ 4045(2)	14(6)			
p 762(14)	0.10(3)	9.1(22)		
p 853(18)	0.013(13)	1.2(12)	3(2)	
p 978(15)	1.08(14)	100(4)	100(2)	100
p 1175(19)	0.018(7)	1.7(6)	3(2)	
p 1521(20)	0.15(3)	13.6(14)	23(6)	11(5)
p 1688(22)	0.043(9)	3.9(7)	10(3)	
p 1825(23)	0.096(16)	8.8(11)	13(4)	
p 2075(30)	0.014(5)	1.3(5)	7(3)	
p 2217(30)	0.044(10)	4.1(8)	6(3)	
p 2299(30)	0.016(6)	1.5(5)		
p 2454(40)*	0.010(4)	1.0(4)		
p 2601(40)*	0.004(3)	0.4(3)		
p 2751(40)*	0.007(4)	0.6(3)		

4 Beta-delayed protons

Beta-delayed protons were observed with the DSSSDs. The ISOLDE Silicon Ball and the thick silicon detectors behind the DSSSDs were used to detect beta particles which triggered the data acquisition. The energy calibration was done as described in sect. 2 and all valid calibrated DSSSDs were summed together. Figure 8 shows a proton spectrum in 20 keV bins. The proton energies agree well with the previous values [6] after adjusting the energy calibration with the peak at 986 keV (see table 3). As this spectrum is measured from a mass-separated source, we can conclude that the earlier controversial proton peaks are indeed from ^{31}Cl and not from ^{25}Si as was claimed in ref. [7].

The biggest surprise in the spectrum is the peak at 762 keV which has not been observed before. This may be due to the fact that the previous experiments had no mass separation and this peak has been identified to belong to the beta decay of ^{32}Cl . The most intense proton peaks from the beta decay of ^{32}Cl are 991(5) keV ($I = 0.0113(17)\%$), 762(5) keV ($I = 0.0052(8)\%$) and 1324(5) keV ($I = 0.0052(8)\%$). As we do not observe any peak at 1324 keV and there are no γ -rays belonging to the mass $A = 32$, this peak must originate from the beta decay of ^{31}Cl . In addition, the proton energy of 762 keV corre-

Table 3. The energy levels of ^{31}S . The proton energies from [5] (989(15) keV, 1528(20) keV) and from [7] (986(10) keV, 1524(10) keV) have been taken into account in the calculations of average proton energies \overline{E}_p and average excitation energies \overline{E}_x . The excitation energies from one- or two-nucleon transfer reactions are from [19] for the states below 7.8 MeV and from [11] for other levels. Peaks smaller than 3σ have been marked with an asterisk.

E_p (keV) This work	E_p (keV) [6]	\overline{E}_p (keV)	E_x (keV) This work	E_x (keV) [6]	E_x (keV) [11,19]	\overline{E}_x (keV) Protons	\overline{E}_x (keV) All
762(14)			6921(15)		6921(25)		6921(13)
853(18)	845(30)	851(16)	7015(19)	7006(30)	6996(15)	7012(16)	7004(11)
978(15)	986(10)	985(6)	7144(16)	7152(10)	7165(9)	7151(6)	7156(5)
1175(19)	1173(20)	1174(14)	7348(20)	7345(20)	7310(11)	7347(14)	7324(9)
1521(20)	1520(15)	1523(8)	7705(21)	7704(15)	7730(12)	7707(8)	7713(7)
1688(22)	1695(20)	1692(15)	7878(23)	7885(20)	7888(25)	7882(15)	7884(13)
1825(23)	1827(20)	1826(15)	8019(24)	8021(20)	7985(25)	8021(16)	8011(13)
2075(30)	2113(30)	2092(20)	8278(30)	8317(30)	8362(25)	8296(21)	8322(16)
2217(30)	2204(30)	2211(20)	8425(30)	8411(30)	8453(25)	8418(21)	8432(16)
2299(30)			8509(30)				
2454(40)*			8669(40)*				
2601(40)*			8821(40)*				
2751(40)*			8977(40)*				

sponds to a known state at 6921(25) keV in ^{31}S which has been observed via $^{29}\text{Si} + ^3\text{He}$ reactions [11] (see table 3).

The excitation energies of ^{31}S were calculated from proton energies in the centre-of-mass frame with a proton separation energy of 6133.0(15) keV and the latest mass values from ref. [1]. Assuming that every decay goes to the ^{30}P ground state, energy levels in agreement with the values from one- or two-nucleon transfer reaction data [11, 19] are obtained. Beta-delayed alphas to the ^{27}Si were considered as negligible due to a high alpha separation energy of 9085.3(15) keV [1]. The measured energies were averaged with the values from earlier beta decay experiments [5–7] and with the levels from transfer reactions [11, 19] (see table 3). The energies from beta decay experiments agree quite well with the energies from the transfer reactions except for the levels at 7347 keV and 8296 keV. The weighted averages of 7156(5) keV and 7713(7) keV levels are in agreement with the values from one-nucleon pickup reactions by Vernotte *et al.* [10], 7156(5) keV and 7725(5) keV. The latter level is suggested to be a multiplet of levels [10].

5 Branching ratios

In the estimation of beta decay branchings to the gamma-decaying states, a few things had to be considered. Firstly, we had only one HPGe detector and thus γ - γ coincidences could not be checked. Secondly, the beta background was minimised by vetoing with the silicon detector in front of the HPGe detector. Although the veto condition revealed most of the interesting γ -peaks hidden in the background, it removed also some relevant counts from the peaks due to random coincidences between beta particles and γ -rays. In order to obtain the real number of counts for a peak visible only in the vetoed spectrum, the peak was scaled

based on the 1266 keV γ -peak from the ^{31}S beta decay. The intensity ratio of the non-vetoed peak to the vetoed peak was 1.566(15). A very similar ratio of 1.56(3) was obtained with the 3134 keV gamma peak of ^{31}S .

Previously, beta decay branching to the 7156 keV state has been estimated to be 0.44% based on the effective production cross-section ratio of ^{31}Cl and ^{32}Cl at 45 MeV and 28 MeV and as given by the ALICE code [6]. However, the latest ENSDF files give a branching of 0.40(1)% to the 7.15 MeV state and 0.04(2)% to the 7.71 MeV state. This is based on ref. [7] which claims that these are the only proton-emitting levels in ^{31}S . In some of the older ENSDF files the branching of 0.44% has been taken as the total proton branching although an overall proton branching of about 0.7% is given in ref. [6]. In this work, absolute beta branchings were obtained by fixing the intensity of the 978 keV protons to 0.44(3)%. This yielded a total proton branching of 0.65(5)%. Table 2 shows the relative intensities for protons and gammas (100% for the 2235 keV gammas) and for protons (100% for the 978 keV protons). The difference between the relative proton peak intensities of ref. [6] and this work may be explained by the lack of mass separation and possible unidentified activities in the previous work.

The absolute branchings are given in fig. 9. The branching to the IAS has been estimated to about 24.3% with a complete sd -space shell model [20]. In a similar manner, a pure single-particle estimate for the Gamow-Teller decay probability of the IAS was used in ref. [4] and a $\log ft$ of 3.20 and a branching of 23% was obtained. The beta decay from ^{31}Cl ($T_Z = -3/2$) to the ground state of ^{31}S ($T_Z = -1/2$) was estimated with the analogous beta decay of ^{31}Si ($T_Z = +3/2$) to the ground state of ^{31}P ($T_Z = +1/2$) for which a $\log ft$ of 5.52(2) [21] and a beta decay Q -value of 1491.88(19) keV [1] have been measured. The $\log ft$ value for the beta decay of ^{31}Cl to

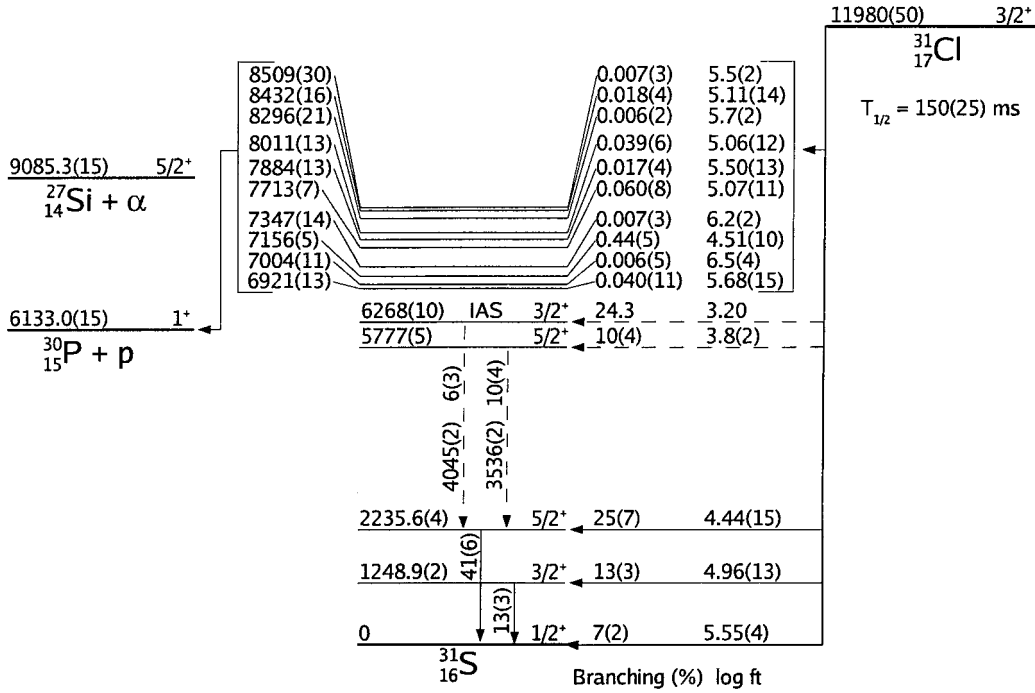


Fig. 9. A beta decay scheme of ^{31}Cl . Only relevant energy levels of ^{31}S are shown. The energies of proton-emitting levels have been averaged with the known values from refs. [5–7, 11] and [19]. The levels at 7347 keV and 8296 keV have been averaged only with the values from beta decay experiments [6, 7] due to too large energy differences to the values of [11] and [19]. The energies of the γ -emitting levels are from ref. [3] except for the 5777(5) keV state [10]. The branching to the ground state is an estimate based on the mirror decay. A theoretical estimation of the branching to the IAS [20] is given together with a single-particle estimate for the $\log ft$ [4]. Spins of the proton-emitting states are ($1/2^+$ – $5/2^+$) except $1/2^+$ for the state at 7004 keV and ($3/2^+$, $5/2^+$) for the state at 7156 keV.

the ground state of ^{31}S was determined with eq. (1) (see ref. [22]):

$$\delta = \frac{ft^+}{ft^-} - 1 \quad (1)$$

$$= 5.2 \times 10^{-3}(W_0^+ + W_0^-) \text{ MeV}^{-1},$$

in which W_0^+ and W_0^- are the total decay energies of the positron and electron decays, respectively.

Equation (1) yielded $\delta = 0.07$ and $\log ft^+ = 5.55(4)$. As in ref. [22], a large error was assumed for δ , $\delta = 0.07 \pm 0.10$. With a $\log f^+ = 5.22(5)$ taken from $\log f$ tables [23] a beta decay branching of 7(2)% was estimated. A very similar procedure was used in ref. [8] in which an upper limit of 78% for the beta decay branching to the 2236 keV state was calculated.

The $\log ft$ values obtained here are between 4.5–6.5 and thus, the observed transitions result most likely from allowed beta decays. Taking into account the ground-state spin of ^{31}Cl , $3/2^+$, spins of $1/2^+$, $3/2^+$ or $5/2^+$ are suggested to these states in ^{31}S . The spin of the state at 6996 keV has been fixed to $1/2^+$, $T = 1/2$ and the state at 7165 keV is ($3/2^+$, $5/2^+$) according to ref. [19]. The state observed at 7015(19) keV has been taken as the 6996 keV state like in ref. [6] but it could also correspond to the state at 7039(10) keV ($3/2^+$, $5/2^+$) [19].

It should be taken into account that if the 3536 keV and 4045 keV transitions do not go to the state at

2236 keV, then the beta decay branching to this state will change. If the 3536 keV gamma transition is excluded, the branching to the 2236 keV state is 35(7)% and the corresponding $\log ft$ value will be 4.29(12). If the feeding from the IAS is neglected, the branching to the 2236 keV state will be 30(7)% and the $\log ft$ 4.35(13). If both transitions are rejected, then the branching and $\log ft$ to the state at 2236 keV will be 41(6)% and 4.23(11), respectively. As a summary, the branching to the state at 2236 keV lies between 25–41% and $\log ft$ is 4.23–4.44.

6 Discussion

Shell model calculations for sd -shell nuclei, such as ^{31}S , have been carried out extensively in the past (see, *e.g.*, [10]). According to the shell model calculations [6] the beta decay of ^{31}Cl has a strong Gamow-Teller feeding to the states around 8 MeV in ^{31}S with a width of about 3–4 MeV. This is in agreement with our observation of beta decay to the proton-emitting states around 7–8 MeV. The calculations [6] also predict small Gamow-Teller decay strengths to the states at 1249 keV and at 2236 keV in agreement with our results. Beta decay feedings to the states around 3 MeV and 4.0–4.5 MeV have also been suggested in [6]. The observed transitions of 3536 keV and 4045 keV fit into this region, but there are no known levels at these energies.

Table 4. A comparison of de-excitation of selected levels in ^{31}S and ^{31}P . The literature values are taken from [21]. The subscripts represent the energies of the final states in keV. The energy and spin assignments marked with an asterisk have been taken from [10].

^{31}S			^{31}P		
E_x (keV)	J^π	E_γ (keV), this work	E_x (keV)	J^π	E_γ (keV) (I_γ (%))
1248.9(2)	$1/2^+$	γ_0 1249.1(14)	1266.15(10)	$3/2^+$	γ_0 1266.12(100)
2235.6(4)	$5/2^+$	γ_0 2234.5(8)	2233.7(2)	$5/2^+$	γ_0 2233.6(100), γ_{1266} 967.5(< 0.1)
5777(5)*	$5/2^{+*}$	γ_{2236} 3536(2)	5892.3(6)	$5/2^{+*}$	γ_{2234} 3658.3(100), γ_{3134} 2758.0(< 11), γ_{3415} 2477.5 (9.9), γ_{1266} 4625.7(< 5.5), γ_0 5891.6(< 5.5), γ_{3295} 2597.1(< 3.3)
6268(10)	$3/2^+$, $T = 3/2$	γ_{2236} 4045(2)	6380.8(17)	$3/2^+$, $T = 3/2$	γ_{2234} 4146.8(100), γ_{3295} 3085.6(22), γ_{1266} 5114.1(20), γ_0 6380.0(20), γ_{3415} 2966.0(< 3.7)

^{31}S provides an opportunity to study mirror energy differences between the states of ^{31}S and ^{31}P (see, *e.g.*, [10]). The 1249 keV and 2236 keV gamma transitions of ^{31}S observed in this work were also detected in [9]. The corresponding mirror states in ^{31}P lie at energies of 1266 keV and 2234 keV (see table 4). Assuming that the observed 3536(2) keV transition goes to the state at 2236 keV, an energy of 5772(2) keV is obtained for the initial state in ^{31}S . This agrees with the previous value of 5777(5) keV [10]. The mirror state of the 5777 keV level is suggested to lie at 5892 keV in ^{31}P [10]. A spin of $5/2^+$ is proposed for these states in ^{31}S and ^{31}P [10] which differs from the spin assignments of ($3/2^+$, $5/2^+$) and $9/2^+$ adopted in [21], respectively. The dominant decay mode of this state at 5892 keV in ^{31}P is to the state at 2234 keV which agrees with our observation of the 3536 keV transition to the state at 2236 keV in ^{31}S .

Based on the mirror states in ^{31}P , one could expect that the IAS in ^{31}S decays dominantly to the state at 2236 keV (see table 4). The decay to the ground state or to the state at 3286 keV (mirror to the state at 3295 keV in ^{31}P) were not observed in this experiment. The decay to the state at 1249 keV could be possible as this peak was observed but the feeding could not be checked due to the lack of γ - γ coincidences. Assuming that the observed γ -transition with an energy of 4045(2) keV is from the IAS to the state at 2236 keV, an energy of 6280(2) keV is obtained for the IAS. This value does not agree with the literature value of 6268(10) keV at 1σ level, but is nevertheless in good agreement with predictions from the isobaric multiplet mass equation (IMME). Namely, IMME with the latest mass values of ^{31}Si , ^{31}P and ^{31}Cl [1] gives an energy of 6278(17) keV for the IAS and the IMME coefficients from ref. [24] yield an energy of 6272(12) keV.

Since the energies and spins of the excited states of ^{31}S have not been known so well, the reaction rate of $^{30}\text{P}(p,\gamma)$ has been calculated using a statistical model calculation (see, *e.g.*, [25]). However, this model requires a relatively high level density and thus, it may not work for such a light nucleus at low temperatures. Most likely single resonances and direct captures will dominate the reaction rate [13]. In order to calculate the reaction rate for indi-

vidual resonances, corresponding resonance energies, spins of the final states and proton and gamma decay widths should be known. In this work, we have found a new proton peak at an energy of 762 keV, confirmed the controversial proton peaks and given spin estimates for these states based on the allowed beta decay. These can be later used for resonance calculations. Nevertheless, the effect on the overall reaction rate is still incomplete, as we did not observe strong beta decay to the IAS. On the other hand, proton captures to the IAS are isospin forbidden and possible only via isospin mixing. This may hinder the strong population to the IAS via reactions other than beta decay. More experiments should be done with high-efficiency HPGe detectors in order to confirm our observation of a possible gamma decay from the IAS combined with novel detectors for detecting low-energy protons from the IAS.

This work has been supported by the European Union Fifth Framework Programme ‘‘Improving Human Potential - Access to Research Infrastructure’’ (Contract No. HPRI-CT-1999-00044) and by the Academy of Finland under the Finnish Centre of Excellence Programme 2000-2005 (Project No. 44875, Nuclear and Condensed Matter Physics Programme at JYFL). A.J. is indebted to financial support from the Academy of Finland (Project No. 46351). D.G.J. acknowledges receipt of an EPSRC Advanced Fellowship. The silicon detectors used in the experiment were provided by the ISOLDE Collaboration and the DSSSDs were from the Aarhus Madrid Collaboration.

References

1. G. Audi *et al.*, Nucl. Phys. A **729**, 337 (2003).
2. W. Benenson *et al.*, Phys. Rev. C **15**, 1187 (1977).
3. P.M. Endt, Nucl. Phys. A **521**, 1 (1990).
4. J. Äystö *et al.*, Phys. Lett. B **110**, 437 (1982).
5. J. Äystö *et al.*, Phys. Scr. T **5**, 193 (1983).
6. J. Äystö *et al.*, Phys. Rev. C **32**, 1700 (1985).
7. T.J. Ognibene *et al.*, Phys. Rev. C **54**, 1098 (1996).
8. L. Axelsson *et al.*, Nucl. Phys. A **634**, 475 (1998).
9. D.G. Jenkins *et al.*, Phys. Rev. C **72**, 031303 (R) 2005.
10. J. Verotte *et al.*, Nucl. Phys. A **655**, 415 (1999).
11. J.M. Davidson *et al.*, Nucl. Phys. A **240**, 253 (1975).

12. J. José *et al.*, *Astrophys. J.* **520**, 347 (1999).
13. J. José *et al.*, *Astrophys. J.* **560**, 897 (2001).
14. J. Äystö, *Nucl. Phys. A* **693**, 477 (2001).
15. L.M. Fraile, J. Äystö, *Nucl. Instrum. Methods A* **513**, 287 (2003).
16. U.C. Bergmann *et al.*, *Nucl. Instrum. Methods A* **515**, 657 (2003).
17. O. Tengblad *et al.*, *Nucl. Instrum. Methods A* **525**, 458 (2004).
18. SRIM2003, <http://www.srim.org/SRIM/SRIM2003.htm>.
19. P.M. Endt, C. Van Der Leun, *Nucl. Phys. A* **310**, 1 (1978).
20. K. Muto *et al.*, *Phys. Rev. C* **43**, 1487 (1991).
21. P.M. Endt, *Nucl. Phys. A* **633**, 1 (1998).
22. J.C. Hardy *et al.*, *Phys. Rev. C* **3**, 700 (1971).
23. N.B. Gove, M.J. Martin, *Nucl. Data Tables* **10**, 205 (1971).
24. J. Britz *et al.*, *At. Data Nucl. Data Tables* **69**, 125 (1998).
25. T. Rauscher, F.K. Thielemann, *At. Data Nucl. Data Tables* **75**, 1 (2000).